Möbius Zn(II)-Hexaphyrins Bearing a Chiral Coordinating Arm: A Chiroptical Switch Featuring P/M Twist Inversion Controlled by Achiral Effectors

Hervé Ruffin, Arnaud Fihey, Bernard Boitrel, Stéphane Le Gac

RESEARCH ARTICLE

Möbius Zn(II)-Hexaphyrins Bearing a Chiral Coordinating Arm: A Chiroptical Switch Featuring P/M Twist Inversion Controlled by Achiral Effectors.

Hervé Ruffin,[a] Arnaud Fihey,[a] Bernard Boitrel*[a] and Stéphane Le Gac*[a]

[a] Dr. H. Ruffin, Dr. A. Fihey, Dr. B. Boitrel, Dr. S. Le Gac
Univ Rennes, CNRS, ISCR (Institut des Sciences Chimiques de Rennes)–UMR 6226, Rennes F-35000, France.
E-mail: bernard.boitrel@univ-rennes1.fr, stephane.legac@univ-rennes1.fr

Supporting information for this article is given via a link at the end of the document.

Abstract: By their conformational flexibility, Möbius aromatic hexaphyrins provide a dynamic chirality attractive to develop stimuli responsive systems such as chiroptical switches. A regular [28]hexaphyrin has been equipped with a chiral coordinating arm to achieve transfer of chirality from a fix stereogenic element to the dynamic Möbius one. The arm allows straightforward formation of labile monometallic Zn(II) complexes with an exogenous ligand, either a carboxylato or an amino with opposite *inwards*/*outwards* orientations relative to the Möbius ring. As a corollary, the chiral coordinating arm is constrained over the ring or laterally, inducing opposite *P* and *M* Möbius configurations with unprecedented high stereoselectivity (diast. excess greater than 95 %). By tuning the transfer of chirality, these achiral effectors generate electronic circular dichroism spectra with bisignate Cotton effect of opposite signs. Switching between distinct chiroptical states was ultimately achieved in mild conditions owing to ligand exchange, with high robustness (10 cycles).

Introduction

Following the pioneering works of Walba (1982)[1] and Herges (2003),[2] the challenging synthesis of Möbius-shaped molecules has received an ever-growing interest.[3,4] Especially, organic compounds exhibiting a π-conjugated Möbius system were not only intriguing as not found in nature, but were also targeted for fundamental understanding of aromaticity. Indeed, 4n Möbius π systems were predicted to gain in stability *vs.* their planar counterparts,[5] a phenomenon now called Möbius aromaticity. Over the last-two decades, extensive work in the chemistry of expanded porphyrins[6] led to significant progresses in experimental investigation of Möbius π systems, unravelling fascinating properties.[7]

Möbius rings are inherently chiral objects (topological chirality),[3b] mirror images being generated by twisting the Möbius band according to a right or a left screw sense (respectively *P* and *M* configurations, Figure 1a top). Compared to other sources of chirality,[8] Möbius chirality has been scarcely investigated at the molecular level and thus constitutes an innovative stereogenic element. Chirality is an important added value to π-conjugated systems opening to a wide range of functions with potential technological applications.[9] Therefore, Möbius π-systems generally exhibiting marked chiroptical activity strongly deserve to be investigated. Particularly, considering the importance of chiroptical switches in many fields of science,[10] designing Möbius-type chiroptical switches represents a real challenge with great opportunities.

Currently, a major obstacle remains the asymmetric preparation of Möbius compounds with only two examples described in the literature. In 2010, the group of Osuka pioneered the enantioselective preparation of a Möbius aromatic [28]hexaphyrin Pd(II) complex with a modest 23% enantiomeric excess (*ee*) (33% yield, Figure 1b top left).[7i] More recently, Tanaka et al. reported the enantioselective synthesis of a non-aromatic Möbius-shaped cycloparaphenylene with a moderate 58% *ee* (52% yield).[4d] These two strategies rely on stereochemically stable Möbius ring, $P \leftrightarrow M$ equilibrium being precluded by metal coordination and by a double stranded motif, respectively.

Focusing on the Möbius [28]hexaphyrin scaffold (Figure 1a), our group has investigated a different approach for chirality induction taking advantage of the dynamic character of the twisted π system. Indeed, this conformationally flexible scaffold undergoes rapid $P \leftrightarrow M$ equilibrium in solution,[7f,g] thus exhibiting a dynamic Möbius chirality (Figure 1a). This feature enables a transfer of chirality from an exogenous stereogenic source under thermodynamic control, useful to build up adaptative molecular systems. In particular, Möbius Zn(II) metallo-receptors exhibiting a strong interplay between aromaticity, guest recognition, and chirality transfer have been developed by our group (Figure 1b).[11] These metal complexes are labile with both exogenous ligand binding and hexaphyrin conformational isomerism being dynamic processes in solution at room temperature. *P/M* twist stereoselectivity can thus be readily controlled *in situ* under mild conditions upon addition of an adequate source of chirality, possibly combined to the cooperative action of an achiral effector (diastereomeric excess [*de*] up to 77%).[11a] Recently, several interconversions between Möbius chiroptical states, eventually of opposite *P/M* helicity, were further achieved *in situ* owing to a chemical trigger, paving the way to Möbius-type chiroptical switches.[11e]

In the present contribution, we have extended our dynamic approach to a different situation, where a source of fix chirality is part of a covalently attached coordinating arm (Figure 1c). We devised a strategy in which the arm is attached at the 2-position of a *meso* phenyl substituent, to be oriented towards the N-core of the hexaphyrin. Targeting a carboxylic acid function, a simple ring opening of a chiral cyclic anhydride was chosen, allowing the simultaneous introduction of a CO_2H function and stereogenic centers. The synthesis of a new AB_5-type hexaphyrin platform,

bearing a single 2-nitrophenyl *meso*-substituent, was thus developed (Scheme 1).

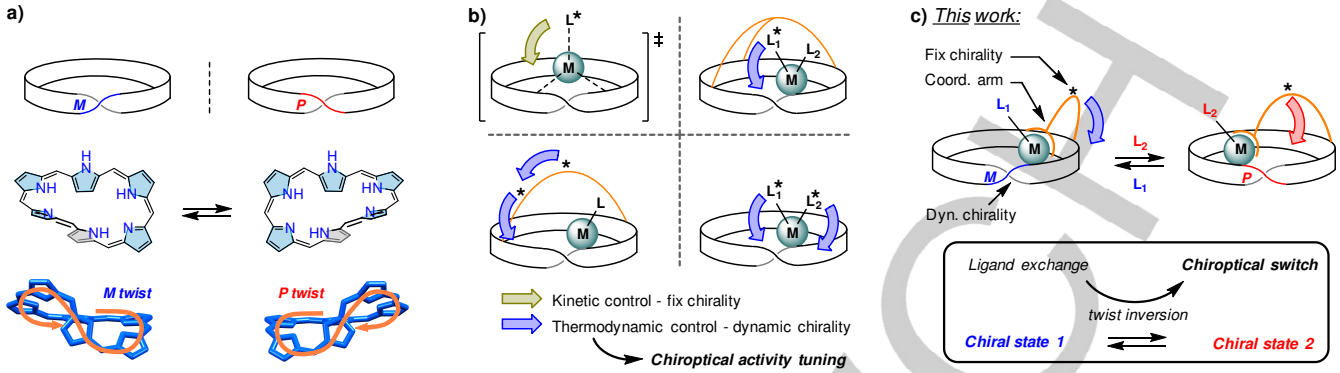

Figure 1. (a) Top: the two enantiomers of a Möbius band (singly twisted) and equilibrium between those of a regular Möbius [28]hexaphyrin. (b) Different approaches for chirality induction with Möbius [28]hexaphyrins: transfer of chirality from an exogenous source of chirality at the transition state of a metal insertion process [top left, M = Pd(II)],[7l] or transfer of chirality with labile Zn(II) complexes, under the influence of cooperative ligand binding.[11a,c-e] (c) Tunable transfer of chirality with a Möbius [28]hexaphyrin functionalized with a chiral coordinating arm, leading to a chemically controlled chiroptical switch (this work).

Results and Discussion

1. Synthesis and characterization of the ligands

Following a recent approach,[11a] we have prepared a new [26]hexaphyrin incorporating respectively one and five 2-nitrophenyl and pentafluorophenyl *meso*-substituents (**1**, Scheme 1). The synthesis of **1** was attempted *via* a macrocyclisation reaction starting from a 3:2:1 mixture of 5-(pentafluorophenyl)dipyrromethane, pentafluorobenzaldehyde and 2-nitrobenzaldehyde. According to established procedures,[11a,12] addition of a catalytic amount of methanesulfonic acid (MSA) in CH_2Cl_2 followed by 2,3-dichloro-5,6-dicyano-1,4-benzoquinone (DDQ) oxidation, led to **1** in 3 % yield after silica gel flash chromatography purification, along with other expanded porphyrins. **1** is a mixture of two rectangular isomers in equilibrium,[13,14] with the 2-nitrophenyl *meso*-substituent located on the long or short side of the rectangle (Scheme 1). The reduction of the nitro function of **1** was catalysed by Pd(0) under a high pressure of hydrogen, and the crude intermediate amino compound was reacted with an excess of either (+) or (-)-*trans*-1,2-cyclohexane dicarboxylic anhydride in THF giving, after silica gel chromatography purification, the targeted compounds ***RR*-4** and ***SS*-4** in good yields, respectively (57 % and 53 %, Scheme 1). Aiming at a related compound with an achiral arm, the crude amino intermediate was also acylated with methyl succinyl chloride, giving hexaphyrin **2** in 44 % yield. Upon Lewis acid cleavage of the methyl ester function, the desired hexaphyrin **3** was obtained in 55 % yield (Scheme 1).

High resolution mass spectrometry (HRMS) characterization indicated a [26]π-conjugated circuit for **1**, whereas **2**, **3**, ***RR*-4** and ***SS*-4** exhibit a reduced [28]π-conjugated circuit formed during the reduction step of the nitro function of **1**. Electronic absorption spectra of **1**-**4** exhibit characteristic features of aromaticity, with a sharp and intense Soret-like band at 567 nm (**1**) or *ca.* 596 nm (**2**-**4**), and Q-like bands up to 1050 nm (Figure S1), in agreement with aromatic planar and Möbius conformations, respectively.

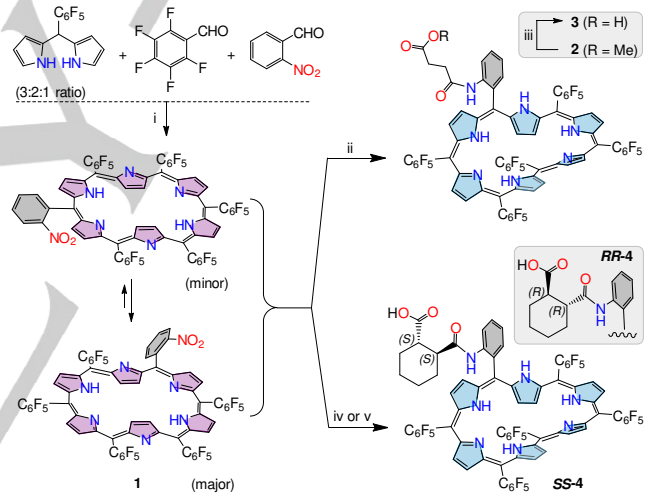

Scheme 1. Synthesis of Möbius [28]hexaphyrins with a (chiral) coordinating arm: (i) MSA cat., CH_2Cl_2, 0°C, 1 h, then DDQ, RT, 1 h (**1**, 3 %); (ii) H_2 (80 bar), Pd(0)/C cat., AcOEt, RT, 15 h; then methyl succinyl chloride, TEA, THF, 0 °C, 1 h (**2**, 44 %); (iii) $AlCl_3$, Et_2S/CH_2Cl_2, 40 °C, 15 h (**3**, 55 %); (iv) (+)-*trans*-1,2-cyclohexane dicarboxylic anhydride, DMAP cat., TEA, THF, RT, 16 h (***RR*-4**, 57 %); (v) (-)-*trans*-1,2-cyclohexane dicarboxylic anhydride, DMAP cat., TEA, THF, RT, 16 h (***SS*-4**, 53 %). For the sake of clarity, only one possible Möbius isomer is depicted.

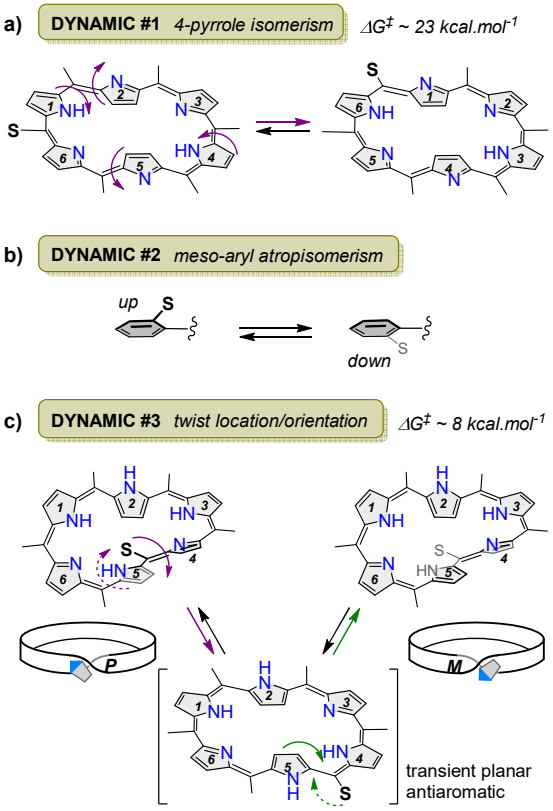

Figure 2. Dynamic processes common to regular hexaphyrins (S = substituent).

An AB_5-type Möbius hexaphyrin, bearing a single 2-modified phenyl *meso*-substituent, leads up to 24 putative Möbius stereoisomers linked by convoluted interconversion pathways (Figure 2 and Figure S0). Three levels of dynamics are combined in these compounds, affecting the position and orientation of the arm (Dynamic #1 and #2), and the position and orientation of the twist (Dynamic #3):

(i) Dynamic #1 (Figure 2a) refers to a 4-pyrrole isomerism process, where two *inner* pyrroles and two *outer* pyrroles invert their orientations.[13,14] A relatively high energy barrier of 23 kcal.mol^{-1} was estimated in the case of a triply linked [26]hexaphyrin.[14]

(ii) Dynamic #2 (Figure 2b) refers to atropisomerism of the 2-modified phenyl *meso*-substituent, adopting either "*up*" or "*down*" orientation relative to the hexaphyrin mean plane.

(iii) Dynamic #3 (Figure 2c) refers to the twisting process of an *inner* pyrrole, leading to the inherently chiral Möbius conformation. A much weaker energy barrier of 8 kcal.mol^{-1} was estimated in the case of *meso*-hexakis(pentafluorophenyl)[28]hexaphyrin.[7f,g]

^{1}H NMR spectra of **3** and ***RR(/SS)*-4** (Figure 3) are dissymmetric and rather well-defined at respectively 330 and 350 K, and correspond to Möbius aromatic conformations. Indeed, β-CH signals are split in three different and characteristic regions[7f,11a] due to the diatropic ring current: (i) the "inner" region experiencing an important shielding (δ ~ 0 ppm, two β-CH of the inverted pyrrole); (ii) the "twisted" region experiencing a moderate shielding (δ ~ 5 ppm, two β-CH facing the inverted pyrrole); (iii) the "outer" region experiencing a moderate deshielding (δ ~ 7.5 ppm, eight peripheral β-CH). Variable temperature NMR experiments revealed that **3** and ***RR(/SS)*-4** are subjected to the three levels of dynamics of Figure 2 (see details in the SI, Figures S21,S23,S31), but an accurate determination of the position(s) and orientation(s) of the arm has remained unsuccessful.

***RR*-4** and ***SS*-4** exhibit mirror image ECD spectra featuring respectively negative and positive bisignate Cotton effects, indicating that their π-systems adopt preferentially opposite *M* and *P* Möbius twists (Figure 4, λ_{max} = 624 nm). Quantification of the *P*/*M* stereoselectivity could not be achieved at this stage due to the dynamic nature of the compounds exhibiting broad NMR spectra.[15]

Overall, the dynamic Möbius scaffold virtually allows a coordinating arm to be located and shifted at any *meso* position, giving rise to multiple possibilities for exploring the ring environment.

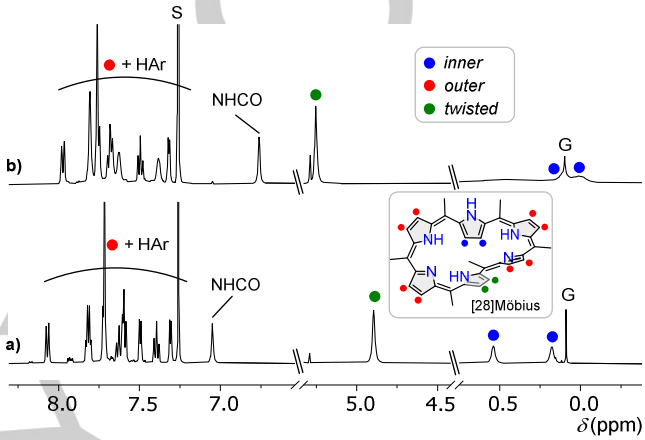

Figure 3. ^{1}H NMR spectra ($CDCl_3$, 500 MHz, selected regions) of (a) **3** (330 K) and (b) ***RR*-4** (350 K). S = solvent, G = grease.

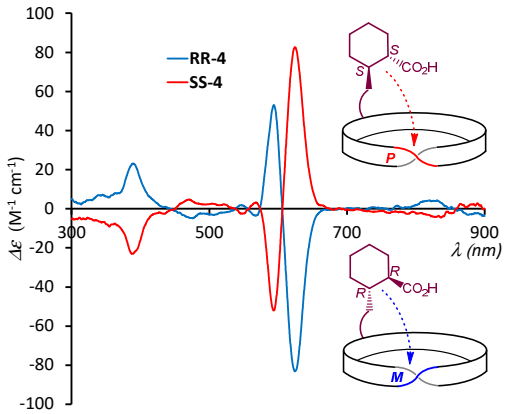

Figure 4. ECD spectra ($CHCl_3$) of ***RR*-4** and ***SS*-4**. Dashed line in cartoon: transfer of chirality.

*2. Zn(II) complexation with **2** and **3** and influence of exogenous carboxylato/amino ligands*

Prior to chirality induction studies, the capability of the coordinating arm to bind zinc in a dynamic way was first evaluated with **2** and **3** by NMR solution analysis. In a 9:1 $CDCl_3/CD_3OD$ mixture, in the presence of N,N-diisopropylethylamine (DIPEA), 1 eq. of $Zn(OTf)_2$ was added to **2** and **3** at room temperature (RT). Whereas nothing happened with **2** (Figure S72), the ^{1}H NMR spectrum of **3** revealed the instantaneous and quasi-quantitative

formation of a Möbius aromatic species (Figure 5b). This difference of behavior is consistent with the formation of a monometallic Zn(II) complex in which the terminal CO_2^- group participates as a σ ligand (**3.Zn**, Scheme 2). Moreover, signals of the four CH_2 succinyl protons are shielded between 0.7 and -0.2 ppm (Figure 5b), indicating that the arm is bent over the *inner* part of the Möbius ring. Based on our previous work (Scheme S1), [11a] zinc is bound "out-of-plane" to the dipyrrin site incorporating the *twisted* pyrrole (depicted in orange in Scheme 2a,b), and the tetrahedral geometry of Zn(II) ensures concomitant binding of *inward* and *outward* ligands. NOE correlations revealed that the arm is located at the *meso* position facing the zinc coordination site (Scheme 2c, details in Figure S52), enabling *inward* coordination of the carboxylato ligand (with a molecule of solvent likely coordinated *outward*). A molecular model of **3.Zn** is depicted in Scheme 2b, illustrating well the orientation of the arm bent over the N-core. Considering 12 possible Möbius stereoisomers differentiable by NMR (Figure S0), the ^{1}H NMR spectrum of **3.Zn** clearly evidences a high stereoselectivity under thermodynamic control.

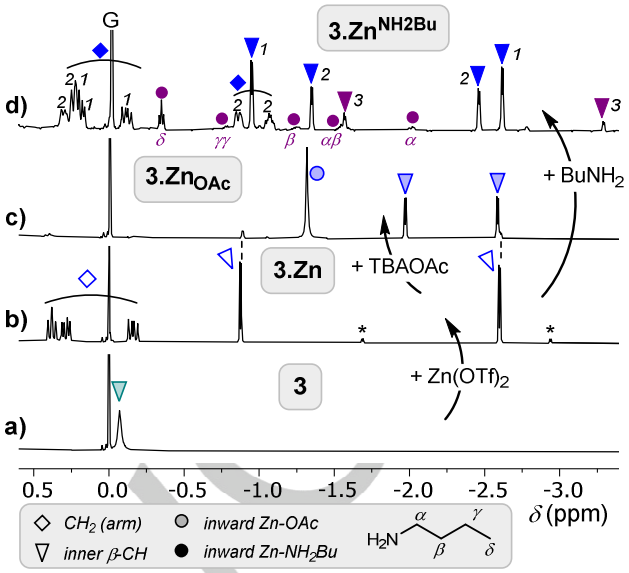

Figure 5. ^{1}H NMR studies related to the complexation of Zn(II) with ligand **3** ($CDCl_3/CD_3OD$ 9:1 with 6 eq. DIPEA, C_0 = 4 mM, 300 K, highfield region): addition of 1 eq. $Zn(OTf)_2$ (b) to **3** (a); addition of 10 eq. of TBAOAc to **3.Zn** (c); addition of 10 eq. of $BuNH_2$ to **3.Zn**, 253 K (d) (* = minor (~5%) unidentified species; G = grease). Labelling *1* to *3* corresponds to three Möbius complexes.

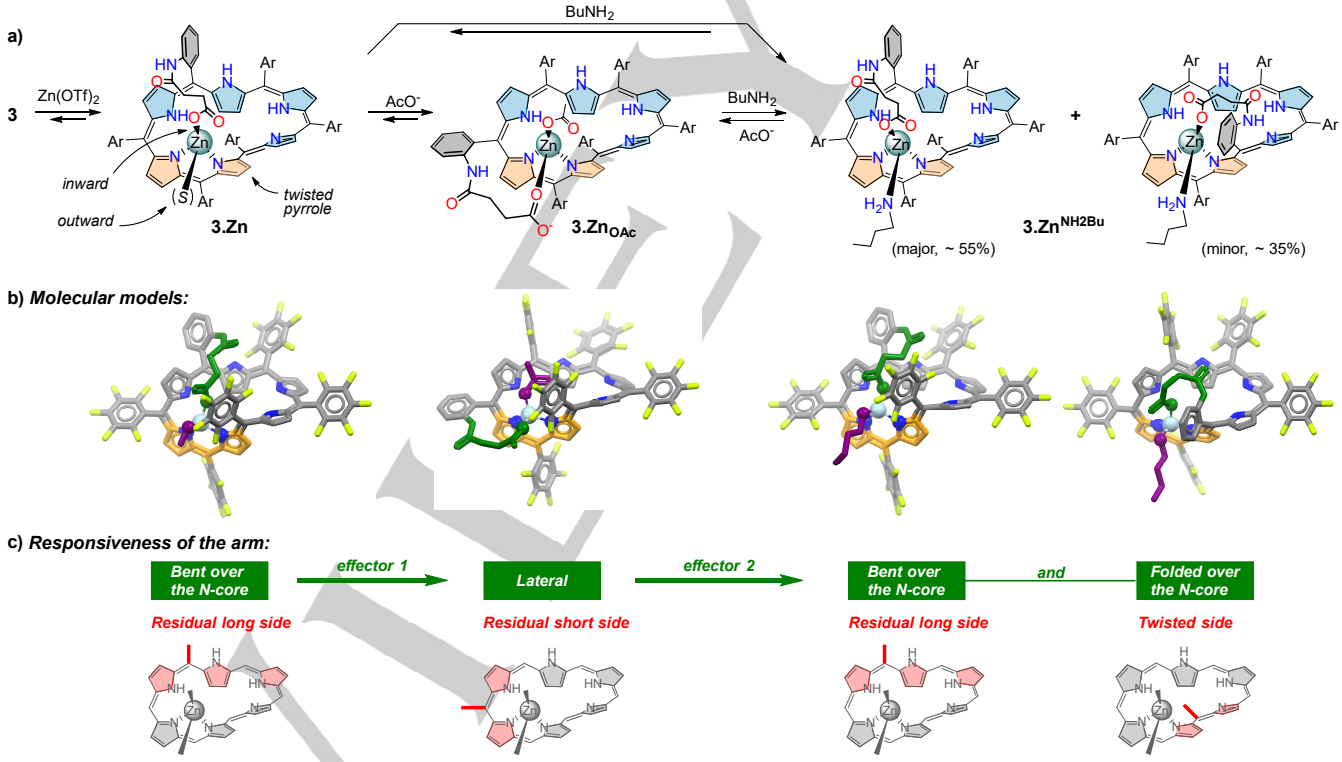

Scheme 2. (a) General overview of Zn(II) complexation with **3**, deduced from NMR solution studies. Conditions: $CDCl_3/CD_3OD$ 9:1, DIPEA. All complexes are racemic, *P* enantiomer is arbitrarily depicted. For **3.Zn**, '(S)' corresponds to the likely coordination of a molecule of solvent, *e.g.* methanol. Counter-ion (*e.g.* TBA^+) of $\mathbf{3.Zn_{OAc}}$ is omitted for clarity. Ar = C_6F_5. In the names $\mathbf{3.Zn_{OAc}}$ and $\mathbf{3.Zn^{NH2Bu}}$, OAc subscripted and NH_2Bu superscripted correspond to *inward* and *outward* coordination, respectively. (b) Molecular models of **3.Zn** (with MeOH coordinated *outward*), $\mathbf{3.Zn_{OAc}}$ (counter-ion omitted), and $\mathbf{3.Zn^{NH2Bu}}$ (two main species) (top views, *P* twist arbitrarily shown; geometry optimization: molecular mechanics performed with UFF force field parameters in Avogadro; *stick* representation except Zn coordination sphere in *ball*, H atoms removed for clarity; F atoms in yellow, N atoms of the hexaphyrin in blue, Zn in light blue, exogenous ligands in purple, coordinating arm in green, dipyrrin binding site in orange). (c) Highlight on changes in the location (in red) and orientation (in green) of the coordinating arm.

Seeking for chemical effectors able to tune the coordination of zinc, the influence of exogenous carboxylato/amino ligands was then investigated through addition of either tetrabutylammonium acetate (TBAOAc) or $BuNH_2$ to **3.Zn**. NMR analysis revealed different behaviors, with the formation of respectively a single and three Möbius complexes (Figure 5c,d and full details in Figure S52):

(i) with the first effector, complex **3.Zn$_{OAc}$** (Scheme 2a) features a shielded ZnOAc moiety oriented towards the Möbius ring, the coordinating arm being located on the residual short side of the ring with a lateral orientation (Scheme 2b and 2c);

(ii) contrastingly, with the second effector, the two main species (**3.Zn^{NH2Bu}**, Scheme 2a) bind a $BuNH_2$ *outward* and exhibit a coordinating arm located on the residual long side and on the twisted side of the ring (Scheme 2c). Their molecular models illustrate two different bent over and folded over orientations of the arm (Scheme 2b).[16]

Besides, in a competition experiment (Figure S73), addition of $BuNH_2$ to **3.Zn$_{OAc}$** led partially to **3.Zn^{NH2Bu}**, suggesting that ligand exchange could be a tool to control the orientation of the arm.

This first entry has shown that exogenous acetato and amino ligands cooperate with the intramolecular carboxylato one, forcing the arm to change its interaction with the metal and thus its position and orientation relative to the N-core, thanks to the dynamic hexaphyrin scaffold (Scheme 2c).[17] As demonstrated hereafter, such a responsiveness is of particular interest for the further control of chirality transfer with the chiral arm of ***RR***(/***SS***)-**4**.

*3. Zn(II) complexation with **RR(/SS)-4** and influence of exogenous carboxylato/amino ligands*

In the next step, chirality induction upon Zn(II) complexation has been investigated with ***RR(/SS)*-4**. $Zn(OTf)_2$ was thus added to ***RR*-4**, ^{1}H NMR spectra revealing instantaneous and quantitative binding of 1 equiv. of metal ion at RT (Figure 6b). The spectrum showed four well-defined patterns in *ca.* 1:1:0.5:0.25 ratio, all characteristics of Möbius aromatic species. This behavior contrasts with **3.Zn** exhibiting a single species with a coordinating arm bent over the N-core. The bulkiness of the cyclohexyl unit may be responsible for a lower selectivity in the location and orientation of the arm, and its chirality *de facto* induces *P*/*M* diastereomers. ECD analysis indicated a shift from a major chiroptical contribution of *M* to *P* twist upon metal complexation (Figure 6 bottom).

The influence of acetato/butylamino ligands was then investigated. First, addition of 5 eq. of TBAOAc led, almost instantaneously at RT, to the quasi-quantitative formation of a single Möbius complex (Figure 6c, Figure S74). In ^{1}H NMR, the presence of an highfield shifted singlet at δ = -1.25 ppm corresponding to a bound AcO^-, together with the lack of shielded cyclohexyl signal, agree with the formation of ***RR*-4.Zn$_{OAc}$** featuring *inward* coordination of ZnOAc and *outward* zinc-binding of the arm (Scheme 3a). By combining different information from NMR and ECD spectroscopies (Figure S69), we determined that the arm is located on the residual short side adjacent to the dipyrrin binding site (Scheme 3c), the twist of *M* configuration (*vide infra*) being localized on the "front side" (Scheme 3a). The lateral orientation of the arm is illustrated by a molecular model of ***RR*-4.Zn$_{OAc}$** (Scheme 3b). The fact that a quasi-single pattern is observed indicates an efficient transfer of chirality responsible for a highly stereoselective formation of a single stereoisomer among 24 possible Möbius isomers (Figure S0). A *de* higher than 90 % can be reasonably estimated based on the NMR spectra (traces of residual signals cannot be integrated or assigned). ECD analysis of ***RR*-4.Zn$_{OAc}$** revealed a negative bisignate Cotton effect corresponding to the quasi-exclusive contribution of a *M* twist (Figure 6 bottom).

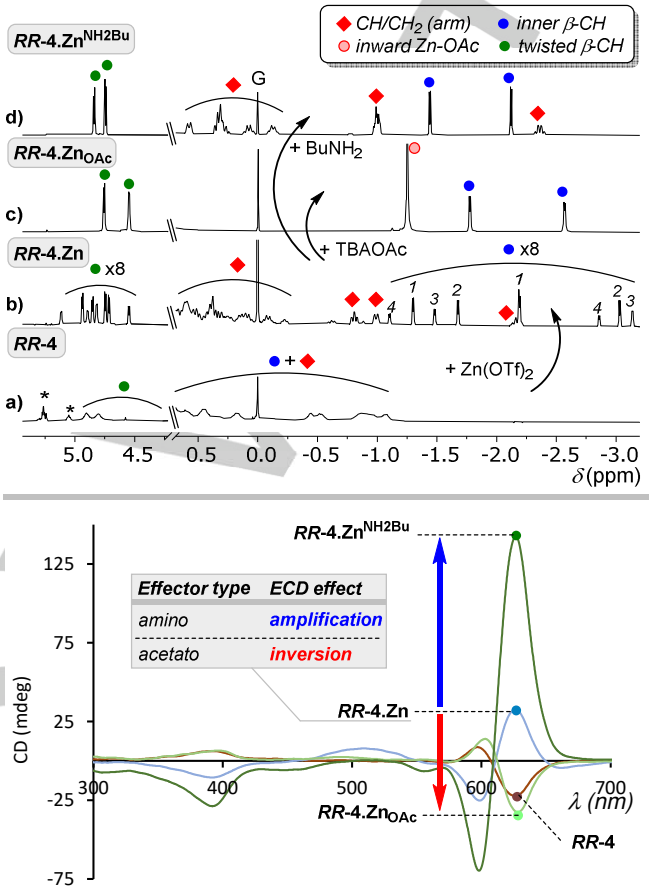

Figure 6. Top: ^{1}H NMR studies related to the complexation of Zn(II) with ligand ***RR*-4** (9:1 $CDCl_3/CD_3OD$, DIPEA, C_0 = 4 mM, 300 K, selected regions); addition to ***RR*-4** (a) of 1.25 eq. of $Zn(OTf)_2$ (b) and either 5 eq. of TBAOAc (c) or 5 eq. of $BuNH_2$ (d); labelling *1* to *4* corresponds to four different Möbius complexes; G = grease, * = impurities. Bottom: changes in the ECD spectra of ***RR*-4** upon addition of $Zn(OTf)_2$, $Zn(OTf)_2$/TBAOAc, and $Zn(OTf)_2/BuNH_2$ (9:1 $CHCl_3/CH_3OH$, DIPEA, C_0 = 30 µM).

Secondly, with 5 eq. of $BuNH_2$, the mixture of complexes ***RR*-4.Zn** was transformed quantitatively and quasi-instantaneously at RT into a single well defined NMR pattern, corresponding to the Möbius complex ***RR*-4.Zn^{NH2Bu}** (Figure 6d, Scheme 3a). In ^{1}H NMR, signals of the cyclohexyl unit are strongly shielded, down to δ = -2.37 ppm, evidencing an *inward* coordination of the arm over the N-core. In contrast, α-CH_2 protons of Zn-NH_2Bu are weakly highfield shifted ($\Delta\delta$ ~ -0.7 ppm), in agreement with an *outward* coordination. Here as well, by combining different information from NMR and ECD spectroscopies (Figure S69), we determined that the arm is located on the twisted side adjacent to the dipyrrin binding site (Scheme 3c), the twist of *P* configuration being localized on the "front side" (Scheme 3a). A molecular model of ***RR*-4.Zn^{NH2Bu}** illustrates the different folded over orientation of the arm *vs* that lateral in the acetato complex (Scheme 3b). As no other species can be seen from both ^{1}H and ^{19}F NMR analysis (Figure S66), a highly efficient transfer of chirality occurs,

estimated greater than 95 % *de*. This is likely one of the highest chirality induction to a Möbius ring reported so far. The formation of ***RR*-4.Zn^{NH2Bu}** led to a drastic increase of the ECD intensity corresponding to the exclusive contribution of a *P* twist. (Figure 6 bottom).

Thus, AcO^- and $BuNH_2$ behave as achiral effectors of different types, leading to opposite effects in ECD spectroscopy. Whereas both effectors afford high *P/M* stereoselectivities, AcO^- induces an inversion of the ECD spectrum whereas $BuNH_2$ amplifies it (Figure 6 bottom). Such a difference relies on their respective preference for *inward* and *outward* coordination to Zn(II) (Scheme 3a), strongly affecting the positioning of the chiral coordinating arm relative to the Möbius hexaphyrin scaffold and the ensuing transfer of chirality.

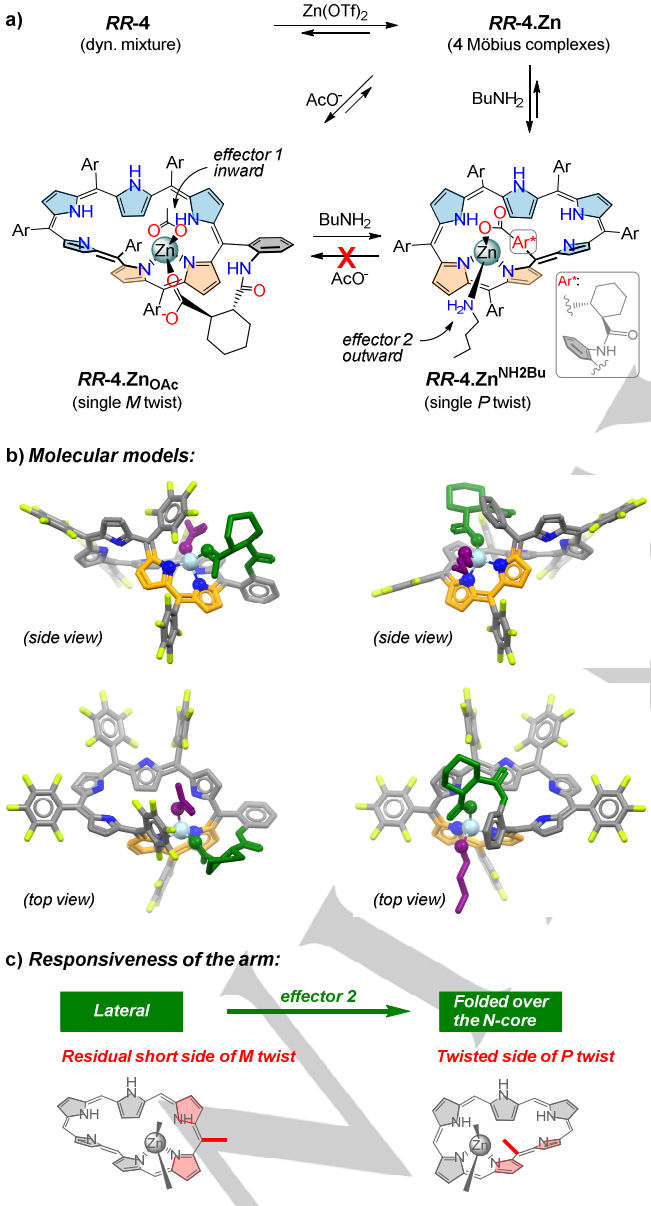

Scheme 3. (a) General overview of Zn(II) complexation with ***RR*-4**, deduced from NMR solution studies. Conditions: $CDCl_3/CD_3OD$ 9:1, DIPEA. Counter-ion (*e.g.* TBA^+) of ***RR*-4.Zn$_{OAc}$** is omitted for clarity. Ar = C_6F_5. (b) Molecular models of ***RR*-4.Zn$_{OAc}$** (*M* twist, counter-ion omitted) and of ***RR*-4.Zn^{NH2Bu}** (*P* twist) [same geometry optimization and representation as in Scheme 2b]. (c) Highlight on changes in the location (in red) and orientation (in green) of the coordinating arm.

TD-DFT calculations performed on these two species led to ECD features in qualitative good agreement with the experimental ones, with a Soret band peaking at *ca.* 610 nm (see the SI). Negative and positive bisignate Cotton effects at the Soret band were obtained for ***RR*-4.Zn$_{OAc}$** and ***RR*-4.Zn^{NH2Bu}** (Figure S83), respectively, in accordance with their assessed *M* and *P* twist configurations. More specifically, this Soret band is for both systems constituted by two electronic transitions with high oscillator strengths, involving the π-conjugated electronic structure of the Möbius skeleton (Figure S82, Table S1). Comparing the localization of the transition densities over the Möbius skeletons did not evidence significant differences between the two compounds, with both oscillator strengths and rotatory strengths found rather similar.

Next, we performed a competition between the two achiral effectors. Whereas the ^{1}H NMR spectrum of ***RR*-4.Zn^{NH2Bu}** was almost unaffected by the addition of TBAOAc, that of ***RR*-4.Zn$_{OAc}$** rapidly transformed at RT (~30 min) into ***RR*-4.Zn^{NH2Bu}** upon addition of $BuNH_2$, without concomitant binding of $BuNH_2$ and AcO^- (Figure S75).[18] The latter ligand exchange conditions enable selective conversion of one chiroptical state to the other, thus defining a forward process of a chiroptical switch.

Continuing to explore the chiroptical response of this system, we performed in the same cuvette the successive additions of different chemicals to ***RR*-4**, and monitored the changes in ECD analysis (Figure S76). Starting from ***RR*-4** in $CHCl_3$, additions of DIPEA, MeOH, $Zn(OTf)_2$, TBAOAc and $BuNH_2$ led to five successive inversions of the sign of the ECD spectra at 626 nm, evidencing a high versatility of the transfer of chirality from the attached chiral coordinating arm.

4. Chemically controlled chiroptical switch

Having in hands effectors inducing reversed chiroptical activity and enabling selective conversion of one chiroptical state to the other, we attempted several switching cycles between the two complexes ***SS*-4.Zn$_{OAc}$** and ***SS*-4.Zn^{NH2Bu}**. To do so, a Boc protection reaction was used as a chemical trigger to release $BuNH_2$ in its Boc-protected form and erase the ECD spectrum of ***SS*-4.Zn^{NH2Bu}**, thus defining a backward process (Figure 7). Such a strategy was recently optimized by our group in the case of related Zn(II) complexes with exogenous chiral ligands.[11e] It proceeds smoothly and selectively, tolerates other functionalities, and generates BuNHBoc and *t*BuOH that do not interfere in the Zn(II) complexation. The chiroptical switching was evidenced by combined ^{1}H NMR and ECD studies (Figure 7, Figures S77-S78). ***SS*-4.Zn$_{OAc}$**, corresponding to State 1, was generated by addition of 1.25 equiv. of $Zn(OTf)_2$ and 5 equiv. of TBAOAc to ***SS*-4**, then 5 equiv. of $BuNH_2$ were added leading to ***SS*-4.Zn^{NH2Bu}** corresponding to State 2 (forward process). Once this first step achieved, 7.5 equiv. of Boc_2O (backward process) and 7.5 equiv. of $BuNH_2$ were alternatively added, leading to successive formations of ***SS*-4.Zn$_{OAc}$** and ***SS*-4.Zn^{NH2Bu}** with good efficiencies. This system is robust with almost no loss of NMR and ECD intensity upon respectively 6 and 10 cycles (Figure 7, Figures S77-S78). The fully reversible inversion of the screw sense of the Möbius π-system, to date unprecedented, affords remarkably large chiroptical changes at 625 nm, ECD values oscillating from +60 mdeg to –160 mdeg. Considering this chemically controlled approach, the covalent attachment sustaining the chiral inductions is a more attractive strategy than our previously

described, less robust systems with exogenous sources of chirality.[11e]

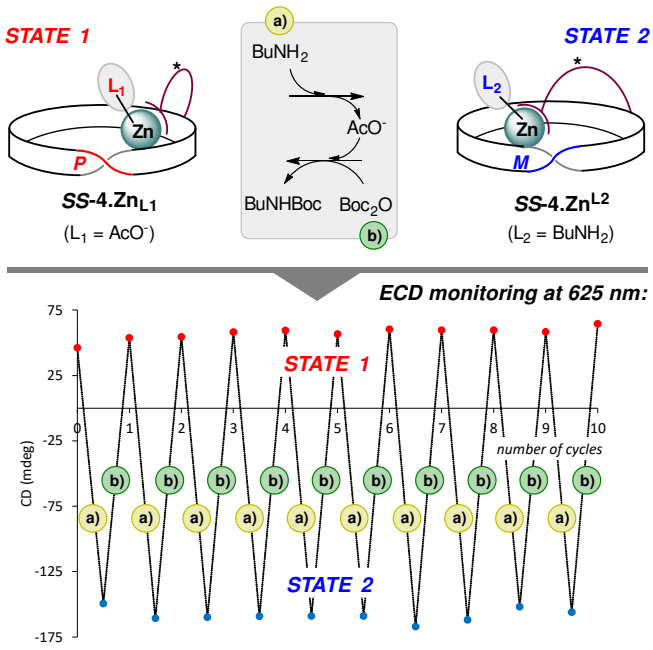

Figure 7. Switching experiment between ***SS*-4.Zn$_{OAc}$** and ***SS*-4.Zn^{NH2Bu}** monitored by ECD spectroscopy (maximum values at 625 nm, $CHCl_3/CH_3OH$ 9:1, DIPEA). a) Forward process: 7.5 eq. $BuNH_2$, 50 °C 10 min; b) backward process: 7.5 eq. Boc_2O, 50 °C 20 min.

Conclusion

New Möbius aromatic [28]hexaphyrin complexes bearing a chiral coordinating arm have been prepared. The Zn(II)-dependent communication between a fix source of chirality and the dynamic Möbius one leads to unprecedented chemically controlled chiroptical switches. The attachment point at the 2 position of a phenyl *meso*-substituent is particularly suited to orient a coordinating function towards the N-core of the ring. By the conformational flexibility of the pyrrolic scaffold and atropisomerism of the *meso*-aryl substituents, the coordinating arm can be virtually located at any *meso* positions with different orientations, enabling full exploration of the Möbius ring environment and ultimately tunable transfer of chirality. Beyond intellectual motivation, the use of the Möbius [28]hexaphyrin scaffold as a chiral switchable unit may find interest in various research fields (sensing, catalysis, optoelectronics, materials,…). More accessible compounds are currently being produced in our laboratory, and other non-invasive triggers (light, redox) controlling the dynamic Möbius chirality are also actively pursued.

Experimental Section

Full experimental details and spectral data are provided in the Supporting Information.

Acknowledgements

We are grateful to the Ministère de l'Enseignement Supérieur et de la Recherche and to the Agence Nationale de la Recherche for financial support (ANR-16-CE07-0014).

Keywords: chiroptical properties • dynamic chirality • Möbius aromaticity • molecular recognition • porphyrinoids

[1] D. M. Walba, M. Richards, R. C. Haltiwanger, *J. Am. Chem. Soc.* **1982**, *104*, 3219-3221.

[2] a) D. Ajami, O. Oeckler, A. Simon, R. Herges, *Nature* **2003**, *426*, 819-821; b) C. Castro, Z. Chen, C. S. Wannere, H. Jiao, W. L. Karney, M. Mauksch, R. Puchta, N. J. R. van Eikema Hommes, P. von Ragué Schleyer, *J. Am. Chem. Soc.* **2005**, *127*, 2425-2432.

[3] a) H. S. Rzepa, *Chem. Rev.* **2005**, *105*, 3697-3715; b) R. Herges, *Chem. Rev.* **2006**, *106*, 4820-4842.

[4] Non-porphyrinoids Möbius rings (see also ref 1,2a): a) G. R. Schaller, F. Topić, K. Rissanen, Y. Okamoto, J. Shen, R. Herges, *Nature Chemistry* **2014**, *6*, 608-613; b) G. Naulet, L. Sturm, A. Robert, P. Dechambenoit, F. Röhricht, R. Herges, H. Bock, F. Durola, *Chem. Sci.* **2018**, *9*, 8930-8936; c) Y.-Y. Fan, D. Chen, Z.-A. Huang, J. Zhu, C.-H. Tung, L.-Z. Wu, H. Cong, *Nature Communications* **2018**, *9*, 3037; d) S. Nishigaki, Y. Shibata, A. Nakajima, H. Okajima, Y. Masumoto, T. Osawa, A. Muranaka, H. Sugiyama, A. Horikawa, H. Uekusa, H. Koshino, M. Uchiyama, A. Sakamoto, K. Tanaka, *J. Am. Chem. Soc.* **2019**, *141*, 14955-14960; e) X. Jiang, S. D. Laffoon, D. Chen, S. Pérez-Estrada, A. S. Danis, J. Rodríguez-López, M. A. Garcia-Garibay, J. Zhu, J. S. Moore, *J. Am. Chem. Soc.* **2020**, *142*, 6493-6498; f) Z. Luo, X. Yang, K. Cai, X. Fu, D. Zhang, Y. Ma, D. Zhao, *Angew. Chem. Int. Ed.* **2020**, *59*, 14854-14860; *Angew. Chem.* **2020**, *132*,14964-14970; g) Z.-L. Qiu, D. Chen, Z. Deng, K.-S. Chu, Y.-Z. Tan, J. Zhu, *Sci. China Chem.* **2021**, *64*, 1004-1008.

[5] E. Heilbronner, *Tetrahedron Lett.* **1964**, *5*, 1923-1928.

[6] a) T. Tanaka, A.Osuka, *Chem. Rev.* **2017**, *117*, 2584-2640; b) Y. Mo Sung, J. Oh, W.-Y. Cha, W. Kim, J. Min Lim, M.-C. Yoon, D. Kim, *Chem. Rev.* **2017**, *117*, 2257-2312; c) B. Szyszko, M. J. Białek, E. Pacholska-Dudziak, L. Latos-Grażyński, *Chem. Rev.* **2017**, *117*, 2839-2909.

[7] Selected early work with Möbius porphyrinoids (see also ref 11): a) M. Stępień, L. Latos-Grażyński, N. Sprutta, P. Chwalisz, L. Szterenberg, *Angew. Chem. Int. Ed.* **2007**, *46*, 7869-7873; *Angew. Chem.* **2007**, *119*, 8015-8019; b) Y. Tanaka, S. Saito, S. Mori, N. Aratani, H. Shinokubo, N. Shibata, Y. Higuchi, Z. S. Yoon, K. S. Kim, S. B. Noh, J. K. Park, D. Kim, A. Osuka, *Angew. Chem. Int. Ed.* **2008**, *47*, 681-684; *Angew. Chem.* **2008**, *120*, 693-696; c) S. Saito, J.-Y. Shin, J. M. Lim, K. S. Kim, D. Kim, A. Osuka, *Angew. Chem. Int. Ed.* **2008**, *47*, 9657-9660; *Angew. Chem.* **2008**, *120*, 9803-9806; d) J. K. Park, Z. S. Yoon, M.-C. Yoon, K. S. Kim, S. Mori, J.-Y. Shin, A. Osuka, D. Kim, *J. Am. Chem. Soc.* **2008**, *130*, 1824-1825; e) E. Pacholska-Dudziak, J. Skonieczny, M. Pawlicki, L. Szterenberg, Z. Ciunik, L. Latos-Grażyński, *J. Am. Chem. Soc.* **2008**, *130*, 6182-6195; f) J. Sankar, S. Mori, S. Saito, H. Rath, M. Suzuki, Y. Inokuma, H. Shinokubo, K. Suk Kim, Z. S. Yoon, J.-Y. Shin, J. M. Lim, Y. Matsuzaki, O. Matsushita, A. Muranaka, N. Kobayashi, D. Kim, A. Osuka, *J. Am. Chem. Soc.* **2008**, *130*, 13568-13579; g) K. S. Kim, Z. S. Yoon, A. Butler Ricks, J.-Y. Shin, S. Mori, J. Sankar, S. Saito, Y. M. Jung, M. R. Wasielewski, A. Osuka, D. Kim, *J. Phys. Chem. A* **2009**, *113*, 4498-4506; h) Z. S. Yoon, A. Osuka, D. Kim, *Nat. Chem.* **2009**, *1*, 113-122; i) T. Tanaka, T. Sugita, S. Tokuji, S. Saito, A. Osuka, *Angew. Chem. Int. Ed.* **2010**, *49*, 6619-6621; *Angew. Chem.* **2010**, *122*, 6769-6771; j) T. Higashino, J. M. Lim, T. Miura, S. Saito, J.-Y. Shin, D. Kim, A. Osuka, *Angew. Chem. Int. Ed.* **2010**, *49*, 4950-4954; *Angew. Chem.* **2010**, *122*, 5070-5074; k) J. M. Lim, J.-Y. Shin, Y. Tanaka, S. Saito, A. Osuka, D. Kim, *J. Am. Chem. Soc.* **2010**, *132*, 3105-3114; l) M. Stępień, B. Szyszko, L. Latos-Grażyński, *J. Am. Chem. Soc.* **2010**, *132*, 3140-3152; m) T. Higashino, B. S. Lee, J. M. Lim, D. Kim, A. Osuka, *Angew. Chem. Int. Ed.* **2012**, *51*, 13105-13108; *Angew. Chem.* **2012**, *124*, 13282-13285.

[8] H. Yamamoto, E. M. Carreira, Comprehensive Chirality; Elsevier Science: Oxford, **2012**.

[9] J. R. Brandt, F. Salerno, M. J. Fuchter, *Nat. Rev. Chem.* **2017**, *1*, 0045.

[10] a) B. L. Feringa, R. A. van Delden, N. Koumura, E. M. Geertsema, *Chem. Rev.* **2000**, 100, 1789-1816; b) L. Zhang, H.-X. Wang, S. Li, M. Liu, *Chem. Soc. Rev.* **2020**, *49*, 9095-9120.

[11] a) H. Ruffin, G. Nyame Mendendy Boussambe, T. Roisnel, V. Dorcet, B. Boitrel, S. Le Gac, *J. Am. Chem. Soc.* **2017**, *139*, 13847-13857; b) S. Le Gac, E. Caytan, V. Dorcet, B. Boitrel, *Org. Biomol. Chem.* **2019**, *17*, 3718-3722; c) R. Benchouaia, N. Cissé, B. Boitrel, M. Sollogoub, S. Le Gac, M. Ménand, *J. Am. Chem. Soc.* **2019**, *141*, 11583-11593; d) B. Boitrel, S. Le Gac, *Chem. Commun.* **2020**, *56*, 9166-9169; e) B. Boitrel, S. Le Gac, *Chem. Commun.* **2021**, *57*, 3559-3562.

[12] M. Suzuki, A. Osuka, *Org. Lett.* **2003**, *5*, 3943-3946.

[13] M. Suzuki, A. Osuka, *Chem. Commun.* **2005**, 3685-3687.

[14] M. Ménand, M. Sollogoub, B. Boitrel, S. Le Gac, *Angew. Chem. Int. Ed.* **2016**, *55*, 297-301; *Angew. Chem.* **2016**, *128*, 305-309.

[15] The attached CO_2H is likely involved in intramolecular H-bonds with pyrroles. Indeed, its protonation state as well as the presence of a polar protic solvent have marked effects on the ECD and NMR spectra of ***RR*-4** (Figures S70,S71).

[16] The minor species labelled "*3*", accounting for ~10%, features an *inward* coordinated $BuNH_2$ as revealed by the important shielding of its alkyl chain (Figure 5d, purple dots).

[17] The driving force remains misunderstood. Possibly, (putative) second spheres of coordination with the amide group of the coordinating arm, as observed in a related system (ref 11a, Scheme S1), might influence the stability of the various complexes and play a role in the Möbius ring reorganization. The influence of Zn(II) coordination on the intimate mechanism remains to be explored as well.

[18] 2D ROESY experiment at 330 K of a 1:1 mixture of ***RR*-4.Zn$_{OAc}$** and ***RR*-4.Zn^{NH2Bu}** revealed selective exchange correlations attesting their interconversion *via* Dynamic #1 process of Figure 2a (Figure S68).

Entry for the Table of Contents

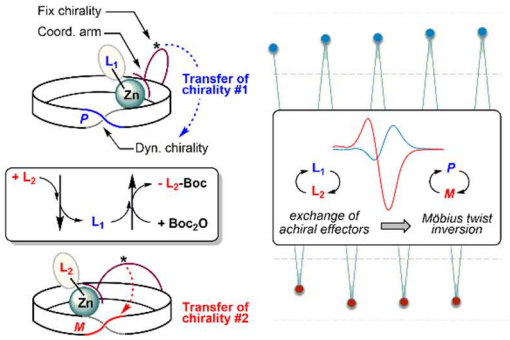

How far the dynamic chirality of Möbius hexaphyrins can be controlled? The answer lies, first, on the capacity of an attached source of chirality to explore the Möbius ring environment, which depends on several convoluted dynamic processes; second, on the responsiveness of the system, making this exploration tunable and *in fine* multi-reversible; third, on the unwavering optimism of the experimenter!